Differential impact of cytoplasmic vs. nuclear RAD51 expression on breast cancer progression and patient prognosis

YEN-YUN WANG[1-3*], KUANG-HUNG CHENG[4,5*], AMOS C. HUNG[6], STEVEN LO[7], PANG-YU CHEN[6], YI-CHIA WU[8-10], MING-FENG HOU[10,11] and SHYNG-SHIOU F. YUAN[2,3,6,12-14]

[1]School of Dentistry, College of Dental Medicine; [2]Drug Development and Value Creation Research Center; [3]Department of Medical Research, Kaohsiung Medical University Hospital, Kaohsiung 807; [4]Institute of Biomedical Sciences, National Sun Yat-Sen University, Kaohsiung 804; [5]Department of Medical Laboratory Science and Biotechnology; [6]Graduate Institute of Medicine, College of Medicine, Kaohsiung Medical University, Kaohsiung 807, Taiwan, R.O.C.; [7]College of Medical, Veterinary and Life Sciences, University of Glasgow, Glasgow G12 8QQ, UK; [8]Division of Plastic Surgery, Department of Surgery, [9]School of Medicine, College of Medicine; [10]Division of Breast Oncology and Surgery, Department of Surgery; [11]Department of Biomedical Science and Environmental Biology, College of Life Science, Kaohsiung Medical University, Kaohsiung 807; [12]Department of Biological Science and Technology, Institute of Molecular Medicine and Bioengineering, Center for Intelligent Drug Systems and Smart Bio-devices (IDS^{2}B), National Yang Ming Chiao Tung University, Hsinchu 300; [13]Translational Research Center; [14]Department of Obstetrics and Gynecology, Kaohsiung Medical University Hospital, Kaohsiung 807, Taiwan, R.O.C.

Received August 25, 2023; Accepted November 14, 2023

DOI: 10.3892/ijo.2023.5600

Abstract. RAD51 recombinase is one of the DNA damage repair proteins associated with breast cancer risk. Apart from its function to maintain genomic integrity within the cell nucleus, RAD51 localized to the cytoplasm has also been implicated in breast malignancy. However, limited information exists on the roles of cytoplasmic vs. nuclear RAD51 in breast cancer progression and patient prognosis. In the present study, the association of cytoplasmic and nuclear RAD51 with clinical outcomes of patients with breast cancer was analyzed, revealing that elevated cytoplasmic RAD51 expression was associated with breast cancer progression, including increased cancer stage, grade, tumor size, lymph node metastasis and chemoresistance, along with reduced patient survival. By contrast, elevated nuclear RAD51 expression largely had the inverse effect. Results from *in vitro* investigations supported the cancer-promoting effect of RAD51, showing that overexpression of RAD51 promoted breast cancer cell growth, chemoresistance and metastatic ability, while knockdown of RAD51 repressed these malignant behaviors. The current data suggest that differential expression of subcellular RAD51 had a distinct impact on breast cancer progression and patient survival. Specifically, cytoplasmic RAD51 in contrast to nuclear RAD51 was potentially an adverse marker in breast cancer.

Correspondence to: Professor Shyng-Shiou F. Yuan, Graduate Institute of Medicine, College of Medicine, Kaohsiung Medical University, 100 Shih-Chuan 1st Road, Sanmin, Kaohsiung 807, Taiwan, R.O.C.
E-mail: yuanssf@kmu.edu.tw

*Contributed equally

Key words: RAD51, breast cancer, subcellular localization, prognosis

Introduction

Breast cancer is leading in terms of cancer incidence and mortality in women worldwide (1). The mainstay of treatment is surgical resection combined with chemo- and/or radiotherapy, plus adjunct hormone therapy depending on the expression of hormonal receptors (2,3). In spite of these established strategies, a proportion of the patients progress to recurrence, metastasis or resistance to cancer therapies, suggesting that additional therapeutic strategies may be required to tailor for individuals (4-6).

RAD51 recombinase has been shown to have a crucial role in the repair of DNA damage, which may occur endogenously from DNA replication stress in fast-growing cancer cells or exogenously due to environmental challenges, including platinum-based chemotherapy and radiotherapy that primarily cause DNA double-strand breaks (7,8). Among pancreatic cell lines, RAD51 expression is lower in irradiation-sensitive CAPAN-1 cells, compared to irradiation-resistant Panc-1 cells (9). In addition, RAD51 overexpression has been reported in cell lines derived from different cancer types and is associated with cellular resistance to irradiation and chemotherapeutic drugs (10,11). As the function of RAD51 in DNA damage repair is well-documented, the majority of research on RAD51 in breast cancer has focused on its expression level in the cell nucleus, e.g. the expression of nuclear RAD51 in breast

tumors has been shown to be positively associated with tumor size and grade (12), as well as lymph node metastasis (13,14). However, discrepancies exist in certain studies, with others finding the expression of nuclear RAD51 in breast tumors inversely associated with grade and local recurrence (15). These findings point towards the possibility of a more elaborate function of RAD51 other than its canonical role in DNA damage repair within the cell nucleus. For instance, increased cytoplasmic RAD51 expression has been found to be a strong risk factor for developing brain metastasis in patients with breast cancer compared to nuclear RAD51 expression (16), and breast tumors expressing high cytoplasmic but low nuclear RAD51 has been associated with adverse breast cancer progression (17).

In the present study, the impact of subcellular RAD51 expression on breast cancer was investigated by analyzing the association of differential RAD51 expression in various subcellular localizations with clinicopathologic and prognostic outcomes in patients with breast cancer. In addition, the roles of differential RAD51 expression in breast cancer cell malignant behaviors were explored *in vitro*.

Patients and methods

Patient specimens. All of the samples used in the present study were de-identified samples from the hospital's biobank added with the informed consent of the patients, but the requirement of informed consent to include them in the present study was waived by the ethics committee. Primary breast tumor specimens had been collected from female patients diagnosed with invasive breast ductal carcinoma and treated with surgical resection at Kaohsiung Medical University Hospital (Kaohsiung, Taiwan) between January 2010 and January 2017. The inclusion criteria were that the patients had no history of cancer and were not simultaneously diagnosed with any other type of cancer, and the exclusion criteria were a diagnosis with benign breast conditions, ductal carcinoma *in situ*, microinvasive carcinoma and rare histological tumor types. The follow-up of the patients after treatment was up to 70 months (median, 41 months). Clinical data used in this study were obtained from the hospital's cancer registry with protocols approved by the Institutional Review Board of Kaohsiung Medical University Hospital [approval nos. KMUH-IRB-20130031 and KMUHIRB-E(I)-20180136] and conducted in accordance with the Declaration of Helsinki.

Immunohistochemistry (IHC). Paraffin-embedded and formalin-fixed tumor sections prepared from the samples taken from surgically treated patients with breast cancer were immunostained with anti-RAD51 antibodies by the Bond-Max automated IHC stainer (Leica Microsystems GmbH) according to the manufacturer's instructions and a previous study by our group (18). The mouse monoclonal antibody against human RAD51 (clone 14B4) for IHC staining was obtained from GeneTex. The images of IHC staining were captured with an Eclipse E600 microscope (Nikon Corp.), followed by quantitation of the IHC staining with categorical scores according to the percentage of positively stained cells (score 1, ≤25%; score 2, 26-50%; score 3, 51-75%; score 4, ≥76%), where samples with scores 1 and 2 were further categorized as low RAD51 expression, and those with scores 3 and 4 were categorized as high RAD51 expression for dichotomized comparisons (18,19). The IHC scoring was evaluated independently by two trained investigators and confirmed by a pathologist.

Cell culture. The human breast cancer cell lines MDA-MB-231 and MCF-7 were purchased from the Bioresource Collection and Research Center (Hsinchu, Taiwan) and maintained in DMEM (Thermo Fisher Scientific, Inc.) supplemented with 10% fetal bovine serum (Biological Industries) and 1% penicillin-streptomycin-amphotericin B solution (Thermo Fisher Scientific, Inc.). The genotypes of these human cell lines were authenticated by short tandem repeat profiling (TopGen Biotechnology).

Gene overexpression and knockdown. Overexpression of RAD51 was conducted by transfecting the breast cancer cell lines with prepackaged lentiviral particles carrying pReceiver-Lv105 vector that expresses full-length human RAD51 (accession no. NM_002875.4) or empty pReceiver-Lv105 vector (GeneCopoeia) as a control. Knockdown of RAD51 was conducted by transfecting the breast cancer cell lines with prepackaged lentiviral particles carrying pLKO.1-puro vector that expresses short hairpin RNA (shRNA) targeting human RAD51 (5'-CGCCCTTTA CAGAACAGACTA-3') or targeting firefly luciferase (5'-GCG GTTGCCAAGAGGTTCCAT-3'; National RNAi Core Facility, Academia Sinica) as a control. The prepackaged lentiviral particles were added to the corresponding cells in their cell culture medium containing 8 μg/ml polybrene (Sigma-Aldrich; Merck KGaA). After 48 h of transfection, 2 μg/ml puromycin (Sigma-Aldrich; Merck KGaA) was added for selection. Surviving cells were continuously maintained in the cell culture medium containing 2 μg/ml puromycin until further experiments.

XTT cell viability assay. MDA-MB-231 or MCF-7 cells were seeded in 96-well plates ($5x10^3$ cells/well) overnight and cultured for 72 h prior to the addition of XTT solution (Sigma-Aldrich; Merck KGaA) according to the manufacturer's instructions. Cell viability was assessed by measuring the optical density (OD) at the main wavelength at 475 nm subtracted by the reference wavelength at 660 nm. To determine the half-maximal inhibitory concentration (IC_{50}), the cells were treated with a series of different concentrations of cisplatin (min. to max., 0-160 μM) for 72 h prior to the addition of the XTT solution followed by readout of the OD as described above. The IC_{50} was calculated using GraphPad Prism 8 (Dotmatics).

Cell cycle distribution. MDA-MB-231 or MCF-7 cells were seeded in 6-well plates ($2x10^5$ cells/well) under normal cell culture conditions. At 80% confluence, the cells were collected and fixed with 75% ethanol (Sigma-Aldrich; Merck KGaA) at -20˚C overnight, followed by staining the DNA contents with propidium iodide/RNase Staining Buffer (BD Biosciences) for 30 min at 37˚C. These cells were then measured with a Cytomics FC 500 flow cytometer (Beckman Coulter), and the distribution of the cell cycle phases was analyzed by WinMDI 2.8 (http://www.cyto.purdue.edu/flowcyt/software.htm).

Transwell migration assay. MDA-MB-231 or MCF-7 cells were plated in Transwell inserts with 8 μm pores ($2x10^4$ cells/insert in 500 μl serum-free cell culture medium per well) of the 24-well plate setting (Corning, Inc.), with the bottom wells containing complete cell culture medium. After 24 h under normal cell culture conditions, the cells remaining on the upper side of the insert were removed with cotton swabs, while those that had migrated to the underside of the insert were fixed with 4% formaldehyde (Sigma-Aldrich; Merck KGaA) for 30 min at room temperature, followed by staining with 0.05% crystal violet (Sigma-Aldrich: Merck KGaA) for 15 min at room temperature. The images of crystal violet staining were captured with an Eclipse Ti Series microscope (Nikon Corp.) and analyzed by ImageJ version 1.53e [National Institutes of Health (NIH)].

Invadopodial invasion assay. MDA-MB-231 cells were plated onto 8-well Nunc Lab-Tek glass chamber slides ($5x10^3$ cells/well; Thermo Fisher Scientific, Inc.) that were pre-coated with Cy3-conjugated gelatin (Merck Millipore) according to the procedures described in the QCM Gelatin Invadopodia Assay (20). After 24 h under normal cell culture conditions, the cells were fixed with 4% formaldehyde (Sigma-Aldrich; Merck KGaA) for 30 min at room temperature, followed by concurrent staining with 2 μg/ml FITC-conjugated phalloidin and 1 μg/ml DAPI for 20 min at room temperature to label filamentous actin (F-actin) and the cell nucleus, respectively. The images of each well were captured by a Zeiss Axioscope fluorescence microscope (Carl Zeiss GmbH) and gelatin degradation was quantified as the degradation area of gelatin normalized to the number of cells using ImageJ (NIH).

Western blot analysis. Protein was extracted using RIPA buffer and the concentration of the protein was measured with a BCA protein assay kit (Pierce™ BCA Protein Assay Kit; ThermoFisher). Equal amounts of total protein extracted from MDA-MB-231 or MCF-7 cells (30 μg/sample) were separated by one-dimensional 10% SDS-PAGE and subsequently transferred to PVDF membranes (PALL Life Sciences) using the Mini-PROTEAN and Trans-Blot systems (Bio-Rad Laboratories, Inc.). The membranes were blocked with 5% non-fat milk (Anchor) for 1 h at room temperature, followed by sequential incubation with primary antibodies overnight at 4˚C and species-matched horseradish peroxidase-conjugated secondary antibodies (Thermo Fisher Scientific, Inc.) for 1 h at room temperature. The signal of immunoreactive proteins was developed in the presence of chemiluminescent reagents (Thermo Fisher Scientific, Inc.) and acquired by the ChemiDoc XRS+ imaging system (Bio-Rad Laboratories, Inc.). The primary antibodies used for western blot were as follows: Mouse monoclonal antibodies against human RAD51 (cat. no. 100469; 1:5,000 dilution; GeneTex), F-actin (cat. no. 205; 1:500 dilution; Abcam) or Lamin A/C (cat. no. 4777; 1:2,000 dilution; Cell Signaling); and rabbit polyclonal antibodies against human RAD51, GAPDH (cat. no. 100118; 1:60,000 dilution; GeneTex) or α-tubulin (cat. no. 112141; 1:5,000 dilution; GeneTex).

Subcellular fractionation and immunoprecipitation. The cytoplasmic and nuclear protein fractions of MDA-MB-231 cells were extracted using the Subcellular Protein Fractionation Kit (Thermo Fisher Scientific, Inc.). Equal amounts of each subcellular fraction (500 μg/sample) were added to 100 ml Protein A Mag Sepharose (Sigma-Aldrich; Merck KGaA) conjugated with 5 μg of the RAD51 antibodies or F-actin antibodies (as specified above) overnight at 4˚C on a rotary tube mixer (Thermo Fisher Scientific, Inc.). The immunoprecipitated protein complex was then separated from the sepharose by boiling for 10 min in Laemmli sample buffer (Bio-Rad Laboratories, Inc.) and subjected to one-dimensional 10% SDS-PAGE for western blot analysis according to the above-mentioned western blot protocol or in-gel digestion of the proteins.

In-gel digestion and liquid chromatography-tandem mass spectrometry (LC-MS/MS). In-gel digestion and protein identification by LC-MS/MS were conducted following previously reported procedures (21). The protein band identified from one-dimensional 10% SDS-PAGE by Coomassie Brilliant Blue R-250 staining (Thermo Fisher Scientific, Inc.) was sliced and de-stained with 25 mM ammonium bicarbonate (Sigma-Aldrich; Merck KGaA) in 50% acetonitrile (Sigma-Aldrich; Merck KGaA) for 1 h at room temperature. The sliced gel was then dehydrated in 100% acetonitrile (Sigma-Aldrich; Merck KGaA) for 5 min and vacuum-dried for 30 min at room temperature. In-gel digestion was conducted in the presence of 0.5 μg trypsin (Sigma-Aldrich; Merck KGaA) dissolved in 25 mM ammonium bicarbonate (Sigma-Aldrich; Merck KGaA) for 16 h at 37˚C. The digested peptide fragments were extracted with 50 μl of a mixture containing 50% acetonitrile (Sigma-Aldrich; Merck KGaA) and 0.1% trifluoroacetic acid (Sigma-Aldrich; Merck KGaA). The extracted peptides were then dissolved in a mixture of 0.1% formic acid (Sigma-Aldrich; Merck KGaA) and 50% acetonitrile (Sigma-Aldrich; Merck KGaA), and analyzed by LC-MS/MS at the Center for Research Resources and Development, Kaohsiung Medical University (Kaohsiung, Taiwan). Protein matching was conducted by a database search for the results of LC-MS/MS spectra with the aid of Mascot (version 2.2; Matrix Science) (https://www.matrixscience.com) (22).

Immunofluorescence. MDA-MB-231 cells grown on 8-well Nunc Lab-Tek II chamber slides (Thermo Fisher Scientific, Inc.) were fixed with 4% paraformaldehyde (Sigma-Aldrich; Merck KGaA) for 30 min at room temperature, followed by incubation of the cells with a permeabilization/blocking buffer containing 0.5% Triton-X 100 (Sigma-Aldrich; Merck KGaA) and 1% bovine serum albumin (Sigma-Aldrich; Merck KGaA) in PBS for 1 h at room temperature. The cells were then sequentially incubated with rabbit polyclonal antibodies against human RAD51 (cat. no. 100469; 1:200 dilution; GeneTex) overnight at 4˚C and Alexa Fluor 555-conjugated donkey polyclonal antibodies against rabbit IgG (cat. no. A32794; 1:500 dilution; Thermo Fisher Scientific, Inc.) for 1 h at room temperature, followed by co-staining with 2 μg/ml FITC-conjugated phalloidin (for F-actin) (cat. no. A12379; Thermo Fisher Scientific, Inc.) and 1 μg/ml DAPI (AAT Bioquest) (for the cell nuclei) for 20 min at room temperature. After the cells were mounted onto coverslips with Mounting Media (Thermo Fisher Scientific,

Inc.), images of the cells were captured by Zeiss Axioscope fluorescence microscope (Carl Zeiss GmbH) and analyzed by ImageJ (NIH).

Statistical analysis. The statistics in this study were analyzed by SPSS (version 25; IBM Corp.) or GraphPad Prism 8 (Dotmatics). Kaplan-Meier survival analysis was conducted to determine disease-free and overall survival of the patients, and differences between survival curves were assessed with the log-rank test. The association between RAD51 expression and clinicopathological parameters was assessed by chi-square test. Hazard ratio (HR) and 95% confidence interval (CI) were derived from Cox regression models. For the *in vitro* studies, the data were presented as the mean ± standard deviation from three independent experiments unless otherwise indicated, and the difference between experimental and control groups was assessed by Student's t-test. $P<0.05$ was considered to indicate a statistically significant difference.

Results

Association of cytoplasmic and nuclear RAD51 expression with clinicopathologic parameters and patient survival in breast cancer. To investigate the association of cytoplasmic (cyto) and nuclear (nu) RAD51 expression with cancer progression, primary tumors obtained from patients with surgically treated breast cancer (age range, 28-86 years; mean ± SD, 51.54±11.42 years) were assessed by IHC (Fig. 1A), and categorical scores were assigned according to the expression levels of RAD51. In general, a heterogeneous expression pattern of RAD51 was observed across the tumor tissues (Fig. 1A). The initial screening was conducted via classification of RAD51 expression into four groups as reported previously (17), including $cyto^{low}/nu^{high}$, $cyto^{high}/nu^{high}$, $cyto^{low}/nu^{low}$ and $cyto^{high}/nu^{low}$ of RAD51 (n=148). Using this analysis, consensus results of the association between subcellular RAD51 expression and breast cancer progression were observed, such as tumor size (P=0.022; Table SI) and disease-free survival of patients with breast cancer (P=0.007; Fig. S1A). In addition to these, the current results revealed that cancer stage and lymph node (LN) metastasis (P=0.001 for both; Table SI) and overall survival of the patients (P=0.025; Fig. S1B) were associated with subcellular RAD51 expression. Overall, significant differences in patient survival, along with other clinicopathological parameters, including tumor size, stage and LN metastasis, were observed among the four patient groups according to their status of subcellular RAD51 expression.

To further compare the roles of differential RAD51 expression in the cytoplasm and in the cell nuclei of breast tumors, independent analyses were performed for patients who were dichotomously grouped into low vs. high expression of cytoplasmic RAD51 (n=224) and nuclear RAD51 (n=180). It was found that the patient group with high cytoplasmic RAD51 expression was associated with increased cancer stage (P=0.003), grade (P=0.035), tumor size (P=0.036) and LN metastasis (P=0.021; Table I). However, the association was the inverse in the patient group with high nuclear RAD51 expression, as it was observed that the patient group with high nuclear RAD51 expression was associated with decreased cancer stage (P<0.001), tumor size (P=0.005) and LN metastasis (P=0.001; Table II). In the survival analysis, the patient group with high cytoplasmic RAD51 expression was associated with poorer disease-free survival (P=0.002; Fig. 1B) and overall survival (P=0.011; Fig. 1C) during a postoperative follow-up period up to 72 months, whereas the patient group with high nuclear RAD51 expression conversely showed positive association with disease-free survival (P=0.003; Fig. 1D) and overall survival (P=0.008; Fig. 1E) compared to their corresponding low RAD51 expression groups. These results suggest the utility of subcellular RAD51 in breast tumor tissues as prognostic markers, with the notion that high cytoplasmic RAD51 expression was adversely associated with breast cancer progression, such as increased cancer stage, tumor size and LN metastasis, along with reduced patient survival; however, high nuclear RAD51 expression had the inverse effect.

The univariate and multivariate Cox regression models were subsequently applied to analyze the utility of parameters of clinicopathologic characteristics and differential RAD51 expression as potential risk factors for patient survival. In the univariate analysis, the parameters showing a strong association with disease-free survival of the patients included cancer stage (II vs. I, P=0.035; III vs. I, P=0.001) and cytoplasmic RAD51 expression (high vs. low, P=0.004) (Table III). In the multivariate analysis, the cancer stage (III vs. I, P=0.012) remained significantly associated with disease-free survival of the patients (Table III). In the univariate analysis for overall survival, the parameters of cancer stage (II vs. I, P=0.026; III vs. I, P=0.006) and cytoplasmic RAD51 expression (high vs. low, P=0.015) also showed a strong association with patient survival, and the association of cancer stage (II vs. I, P=0.048; III vs. I, P=0.017) with overall survival remained significant in the multivariate analysis (Table IV). In these Cox regression models, the association between nuclear RAD51 expression and patient survival was not significant (Tables III and IV), suggesting that cytoplasmic RAD51 expression, rather than nuclear RAD51 expression, represented a more influential risk regarding survival of patients with breast cancer. In addition to these, it was observed that the histologic grade, which is frequently associated with patient outcomes, showed a trend of increasing hazard ratios but did not reach a statistically significant level in the univariate and multivariate analyses (Tables III and IV); this discrepancy may be resolved by further investigation with a larger magnitude of sample size.

Resistance to chemotherapy has been one of the main obstacles in breast cancer management, yet clinical markers to effectively predict responses to chemotherapy are still under exploration (23,24). Therefore, in the present study, the effects of subcellular RAD51 expression on patient survival with regard to chemotherapy was further investigated in these cohorts. As presented in Fig. 2A and C, it was found that high cytoplasmic RAD51 expression was associated with poorer disease-free survival (P=0.010) and overall survival (P=0.040) in the patient group receiving adjuvant chemotherapy, while the association of cytoplasmic RAD51 expression with patient survival was not significant in the patient group without chemotherapy (Fig. 2B and D). An opposite trend was observed in the analysis for nuclear RAD51 expression, where high nuclear RAD51 expression was in favor of disease-free survival (P=0.006) and overall survival (P=0.040) in the

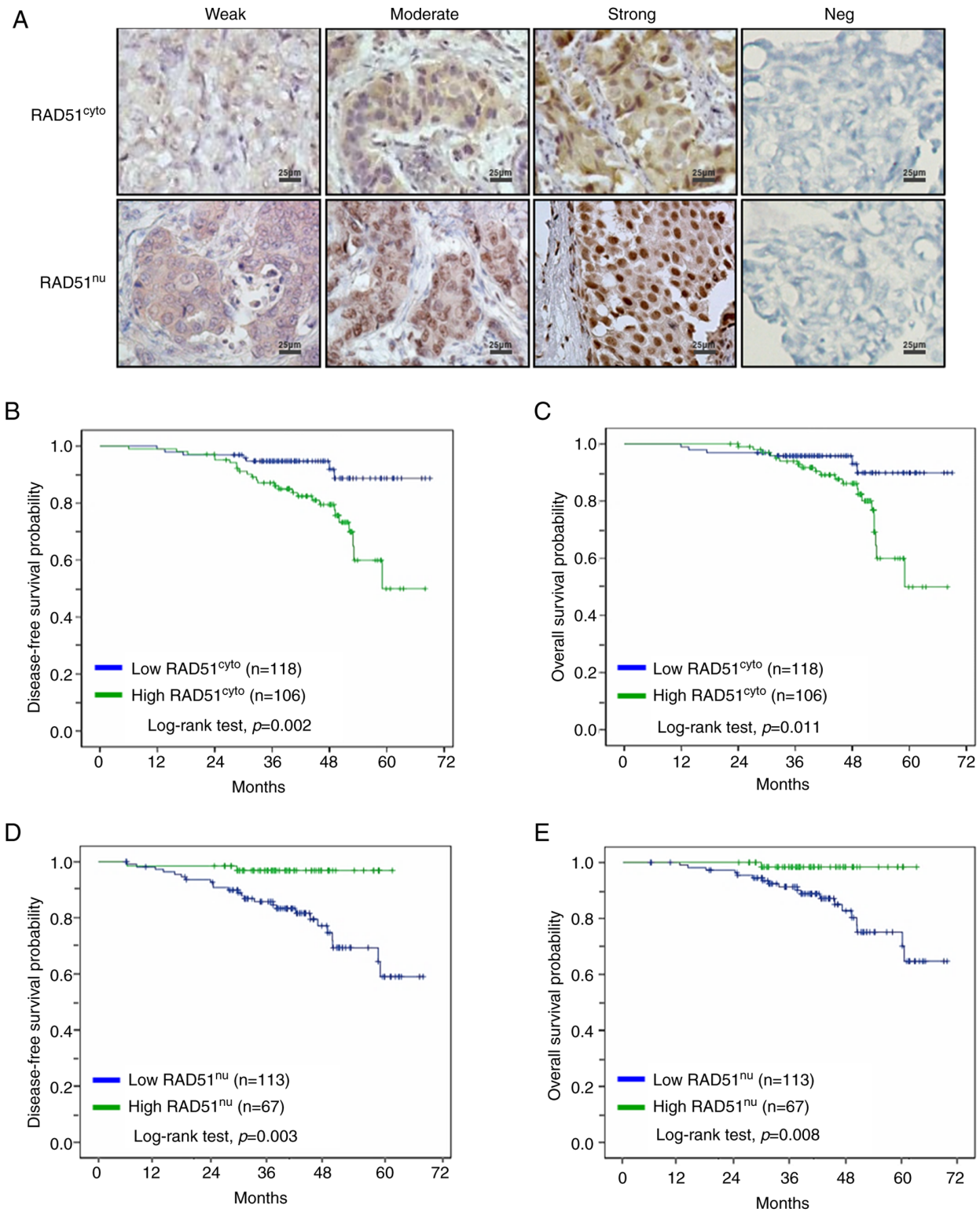

Figure 1. Subcellular RAD51 expression in breast tumors and Kaplan-Meier survival analysis for patients with breast cancer according to differential RAD51 expression. (A) IHC analysis for cytoplasmic RAD51 (RAD51^{cyto}) and nuclear RAD51 (RAD51^{nu}) expression in the primary breast tumor sections with representative examples for different staining intensities. The negative control was prepared under the same conditions except that the primary antibodies were omitted. The IHC images were generated by TissueFAXS Imaging Software 6.0 (TissueGnostics; scale bars, 25 μm). (B) Disease-free survival and (C) overall survival of patients with breast cancer were analyzed for the patient groups of low RAD51^{cyto} expression vs. high RAD51^{cyto} expression, and (D) disease-free survival and (E) overall survival of patients with breast cancer for the patient groups of low RAD51^{nu} expression vs. high RAD51^{nu} expression. The P-values were determined by two-sided log-rank tests. IHC, immunohistochemistry; cyto, cytoplasm; nu, nucleus; Neg, negative.

patient group receiving chemotherapy (Fig. 2E and G), while the significance of association was not observed in the patient group without chemotherapy (Fig. 2F and H). These results indirectly suggest the potential of a different prognostic role of subcellular RAD51 expression in consideration of patients with breast cancer receiving adjuvant chemotherapy.

Table I. Association of cytoplasmic RAD51 expression with clinicopathologic characteristics in patients with breast cancer (n=224).

Variable	Total	Cytoplasmic RAD51 expression		P-value
		Low (n=118)	High (n=106)	
Stage				0.003
I	79 (35.3)	52 (44.1)	27 (25.5)	
II	83 (37.0)	43 (36.4)	40 (37.7)	
III	62 (27.7)	23 (19.5)	39 (36.8)	
Grade				0.035
1	19 (8.4)	15 (12.7)	4 (3.8)	
2	147 (65.6)	77 (65.3)	70 (66.0)	
3	58 (25.9)	26 (22.0)	32 (30.2)	
Age, years				0.139
≤50	111 (49.6)	64 (54.2)	47 (44.3)	
>50	113 (50.4)	54 (45.8)	59 (55.7)	
BMI, kg/m^2				0.671
≤24	128 (57.1)	69 (58.5)	59 (55.7)	
>24	96 (42.9)	49 (41.5)	47 (44.3)	
Tumor size, cm				0.036
<2	114 (50.9)	69 (58.5)	45 (42.4)	
2-5	90 (40.2)	42 (35.6)	48 (45.3)	
>5	20 (8.9)	7 (5.9)	13 (12.3)	
LN metastasis				0.021
No	132 (58.9)	78 (66.1)	54 (50.9)	
Yes	92 (41.1)	40 (33.9)	52 (49.1)	
ER status				0.116
Negative	79 (35.3)	36 (30.5)	43 (40.6)	
Positive	145 (64.7)	82 (69.5)	63 (59.4)	
PR status				0.076
Negative	96 (42.9)	44 (37.3)	52 (49.1)	
Positive	128 (57.1)	74 (62.7)	54 (50.9)	
HER2 status				0.386
Negative	146 (65.2)	80 (67.8)	66 (62.3)	
Positive	78 (34.8)	38 (32.2)	40 (37.7)	

Values are expressed as n (%). The P-values were calculated by the Chi-square test. BMI, body mass index; ER, estrogen receptor; HER2, epidermal growth factor receptor 2; LN, lymph node; n, patient number; PR, progesterone receptor.

Effect of differential RAD51 expression on in vitro breast cancer cell growth and chemoresistance. The roles of differential RAD51 expression on breast cancer cell behaviors were investigated via the following *in vitro* assays. Two widely studied human breast cancer cell lines, MDA-MB-231 (basal type) and MCF-7 (luminal type A) (25), were transfected with lentiviral particles that contain full-length RAD51 for gene overexpression or shRNA targeting RAD51 for gene knockdown (Fig. 3A). The XTT assay to determine cancer cell growth revealed that overexpression of RAD51 enhanced the proliferative ability of these breast cancer cells (Fig. 3B), whereas knockdown of RAD51 reduced their proliferative ability compared to their corresponding controls (Fig. 3C). The cell cycle distribution was further evaluated by flow cytometry, which showed that both MDA-MB-231 and MCF-7 cells with overexpression of RAD51 had an increased proportion of the G2/M phases (Fig. 3D). On the contrary, knockdown of RAD51 led to a reduced proportion of the G2/M phases in these breast cancer cells (Fig. 3E). Taken together, the results suggest that elevation of RAD51 expression promoted breast cancer cell growth, which potentially resulted from the progression of the cell cycle into the G2/M phases.

To investigate whether the differential RAD51 expression is involved in the resistance of breast cancer cells to chemotherapy, the effect of RAD51 overexpression or knockdown on cell growth of the breast cancer cells that were treated with cisplatin, a first-line therapeutics administered in breast and various tumors, was assessed (26). An increased shift of the IC_{50}

Table II. Association of nuclear RAD51 expression with clinicopathologic characteristics in patients with breast cancer (n=180).

Variable	Total	Nuclear RAD51 expression		P-value
		Low (n=113)	High (n=67)	
Stage				<0.001
I	59 (32.8)	25 (22.1)	34 (50.8)	
II	71 (39.4)	50 (44.3)	21 (31.3)	
III	50 (27.8)	38 (33.6)	12 (17.9)	
Grade				0.218
1	14 (7.8)	8 (7.1)	6 (9.0)	
2	119 (66.1)	80 (70.8)	39 (58.2)	
3	47 (26.1)	25 (22.1)	22 (32.8)	
Age, years				0.203
≤50	91 (50.6)	53 (46.9)	38 (56.7)	
>50	89 (49.4)	60 (53.1)	29 (43.3)	
BMI, kg/m^2				0.261
≤24	95 (52.8)	56 (49.6)	39 (58.2)	
>24	85 (47.2)	57 (50.4)	28 (41.8)	
Tumor size, cm				0.005
<2	91 (50.6)	47 (41.6)	44 (65.7)	
2-5	71 (39.4)	51 (45.1)	20 (29.8)	
>5	18 (10.0)	15 (13.3)	3 (4.5)	
LN metastasis				0.001
No	106 (58.9)	56 (49.6)	50 (74.6)	
Yes	74 (41.1)	57 (50.4)	17 (25.4)	
ER status				0.727
Negative	62 (34.4)	40 (35.4)	22 (32.8)	
Positive	118 (65.6)	73 (64.6)	45 (67.2)	
PR status				0.854
Negative	79 (43.9)	49 (43.4)	30 (44.8)	
Positive	101 (56.1)	64 (56.6)	37 (55.2)	
HER2 status				0.503
Negative	121 (67.2)	78 (69.0)	43 (64.2)	
Positive	59 (32.8)	35 (31.0)	24 (35.8)	

Values are expressed as n (%). The P-values were calculated by the Chi-square test. BMI, body mass index; ER, estrogen receptor; HER2, epidermal growth factor receptor 2; LN, lymph node; PR, progesterone receptor.

value of cisplatin was observed in both RAD51-overexpressing MDA-MB-231 cells (Fig. 4A) and MCF-7 cells (Fig. 4B), whereas knockdown of RAD51 resulted in a reduced IC_{50} of cisplatin in these breast cancer cells (Fig. 4C and D). The shift of the IC_{50} for cisplatin treatment further suggests that the differential RAD51 expression may be involved in the regulation of cancer cell growth during chemotherapy, with the notion that resistance to cisplatin treatment occurred in RAD51-overexpressing breast cancer cells.

While the effect of cisplatin treatment on RAD51 subcellular localization has not been previously reported, to the best of our knowledge, it was reported that curcumin induces DNA damage and leads to RAD51 migrating to the nucleus (27). Previous studies also showed that in HeLa and HCT116 cells, RAD51 redistributed from the cytoplasm to the nucleus after exposure to ionizing radiation (28,29). In the current study, it was shown that RAD51 overexpression led to increased cytoplasmic and nuclear RAD51 expression and more surviving cells (chemoresistance) among MDA-MB-231 and MCF-7 cells after cisplatin treatment (Figs. S2 and 4). On the other hand, RAD51 knockdown led to decreased surviving cells (chemosensitivity) in MDA-MB-231 cells after cisplatin treatment. All of these data together suggest that RAD51 expression levels are positively associated chemoresistance and radioresistance in breast cancer cells.

Effect of differential RAD51 expression on in vitro breast cancer cell migration and invasion ability. The effect of RAD51 expression on the *in vitro* metastatic ability of breast cancer cells was investigated by Transwell migration

Table III. Univariate and multivariate Cox regression analyses of disease-free survival in patients with breast cancer.

	Univariate		Multivariate	
Variable	HR (95% CI)	P-value	HR (95% CI)	P-value
Stage				
II vs. I	3.91 (1.10-13.88)	0.035	3.29 (0.91-11.86)	0.069
III vs. I	7.67 (2.26-26.07)	0.001	5.12 (1.44-18.27)	0.012
Grade				
2 vs. 1	2.62 (0.63-10.88)	0.186		
3 vs. 1	2.39 (0.52-10.99)	0.265		
Age (>50 vs. ≤50 years)	1.79 (0.88-3.61)	0.106		
BMI (>24 vs. ≤24 kg/m^2)	1.97 (0.99-3.94)	0.055		
ER positive	0.87 (0.73-1.03)	0.111		
PR positive	0.87 (0.73-1.04)	0.117		
HER2 positive	0.86 (0.67-1.11)	0.254		
Cytoplasmic RAD51 (high vs. low)	3.40 (1.47-7.86)	0.004	2.26 (0.95-5.40)	0.067
Nuclear RAD51 (high vs. low)	0.28 (0.07-1.23)	0.093		

Variables with P>0.05 in the univariate Cox regression analysis were excluded from the multivariate Cox regression analysis. BMI, body mass index; CI, confidence interval; ER, estrogen receptor; HER2, epidermal growth factor receptor 2; HR, hazard ratio; PR, progesterone receptor.

Table IV. Univariate and multivariate Cox regression analyses of overall survival in patients with breast cancer.

	Univariate		Multivariate	
Variable	HR (95% CI)	P-value	HR (95% CI)	P-value
Stage				
II vs. I	5.55 (1.23-25.11)	0.026	4.64 (1.01-21.24)	0.048
III vs. I	8.10 (1.84-35.66)	0.006	6.48 (1.41-29.88)	0.017
Grade				
2 vs. 1	3.48 (0.47-26.10)	0.224		
3 vs. 1	4.80 (0.58-39.86)	0.146		
Age (>50 vs. ≤50 years)	1.79 (0.83-3.89)	0.140		
BMI (>24 vs. ≤24 kg/m^2)	1.78 (0.83-3.81)	0.138		
ER positive	0.87 (0.72-1.05)	0.144		
PR positive	0.85 (0.70-1.03)	0.090		
HER2 positive	0.97 (0.74-1.26)	0.798		
Cytoplasmic RAD51 (high vs. low)	3.10 (1.24-7.71)	0.015	1.88 (0.71-4.94)	0.202
Nuclear RAD51 (high vs. low)	0.21 (0.03-1.64)	0.137		

Variables with P>0.05 in the univariate Cox regression analysis were excluded from the multivariate Cox regression analysis. BMI, body mass index; CI, confidence interval; ER, estrogen receptor; HER2, epidermal growth factor receptor 2; HR, hazard ratio; PR, progesterone receptor.

and invadopodial invasion assays. As presented in Fig. 5A, MDA-MB-231 and MCF-7 cells with overexpression of RAD51 exhibited an increased ability of cell migration. On the contrary, knockdown of RAD51 decreased the cell migration ability of these breast cancer cells (Fig. 5B). In addition to cell migration, increased ability of invadopodial cell invasion was observed in MDA-MB-231 cells with overexpression of RAD51, whereas knockdown of RAD51 repressed the cell invasion ability (Fig. 5C). To further explore the biological activity associated with subcellular RAD51 expression, the cytoplasmic and nuclear proteins from MDA-MB-231 cells with overexpression of RAD51, or those from control cells, were fractionated prior to immunoprecipitation with anti-RAD51 antibodies. The fractionation result showed that endogenous RAD51 is expressed in both the cytoplasm and nuclei of MDA-MB-231 cells and overexpression increased RAD51 expression in both cytoplasm and nuclei (Fig. S2A). After immunoprecipitation with anti-RAD51 antibodies,

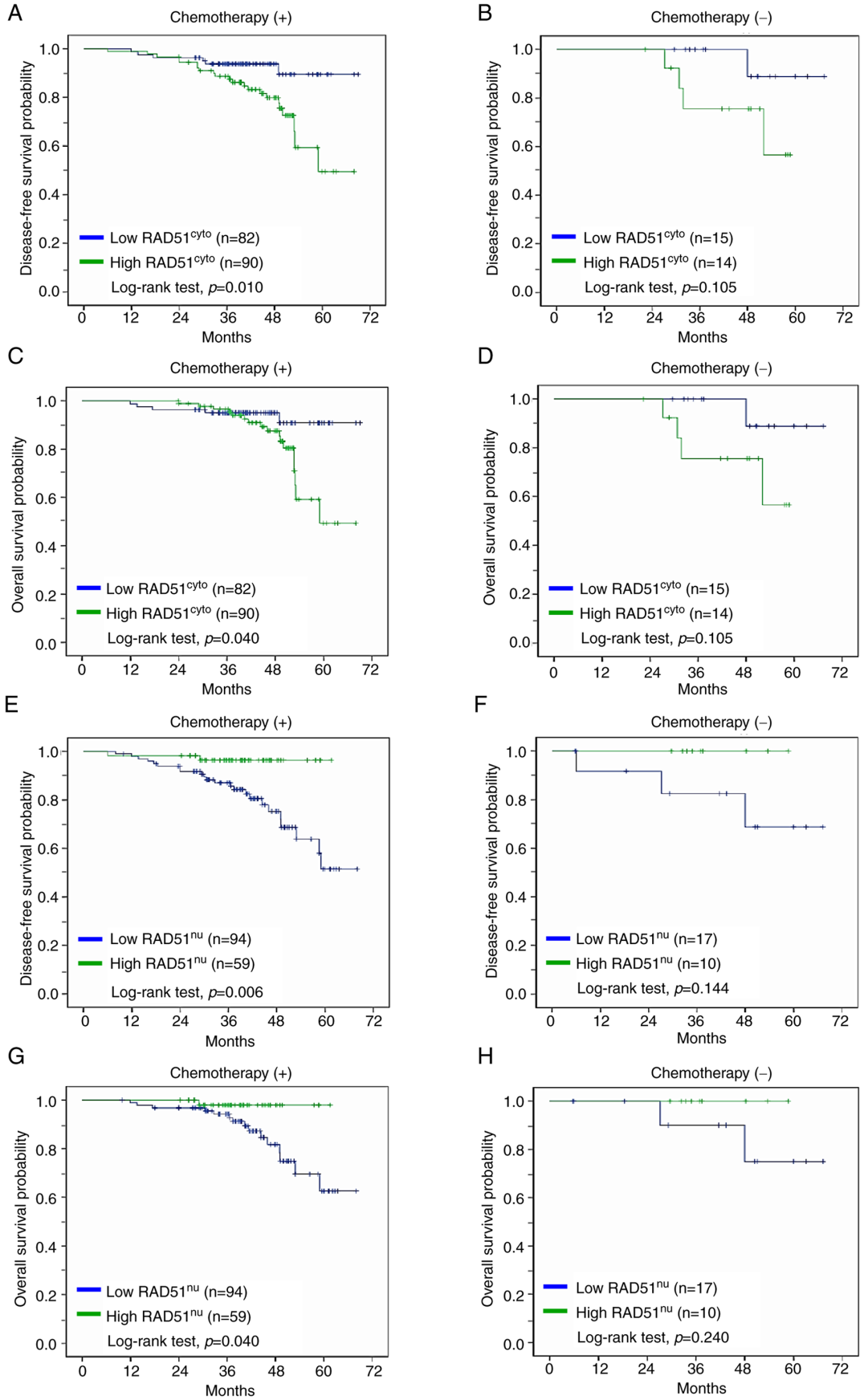

Figure 2. Kaplan-Meier survival analysis for differential RAD51 expression in patients with breast cancer with stratification according to adjuvant chemotherapy. (A) Disease-free survival of patients with breast cancer with chemotherapy (+) and (B) without chemotherapy (-) according to $RAD51^{cyto}$ expression. (C) Overall survival of patients with breast cancer with chemotherapy (+) and (D) without chemotherapy (-) according to $RAD51^{cyto}$ expression. (E) Disease-free survival of patients with breast cancer with chemotherapy (+) and (F) without chemotherapy (-) according to $RAD51^{nu}$ expression. (G) Overall survival of patients with breast cancer with chemotherapy (+) and (H) without chemotherapy (-) according to $RAD51^{nu}$ expression. There were missing data (n=23) in A-D due to the unavailability of the patients' survival information. The P-values were determined by a two-sided log-rank test. cyto, cytoplasm; nu, nucleus.

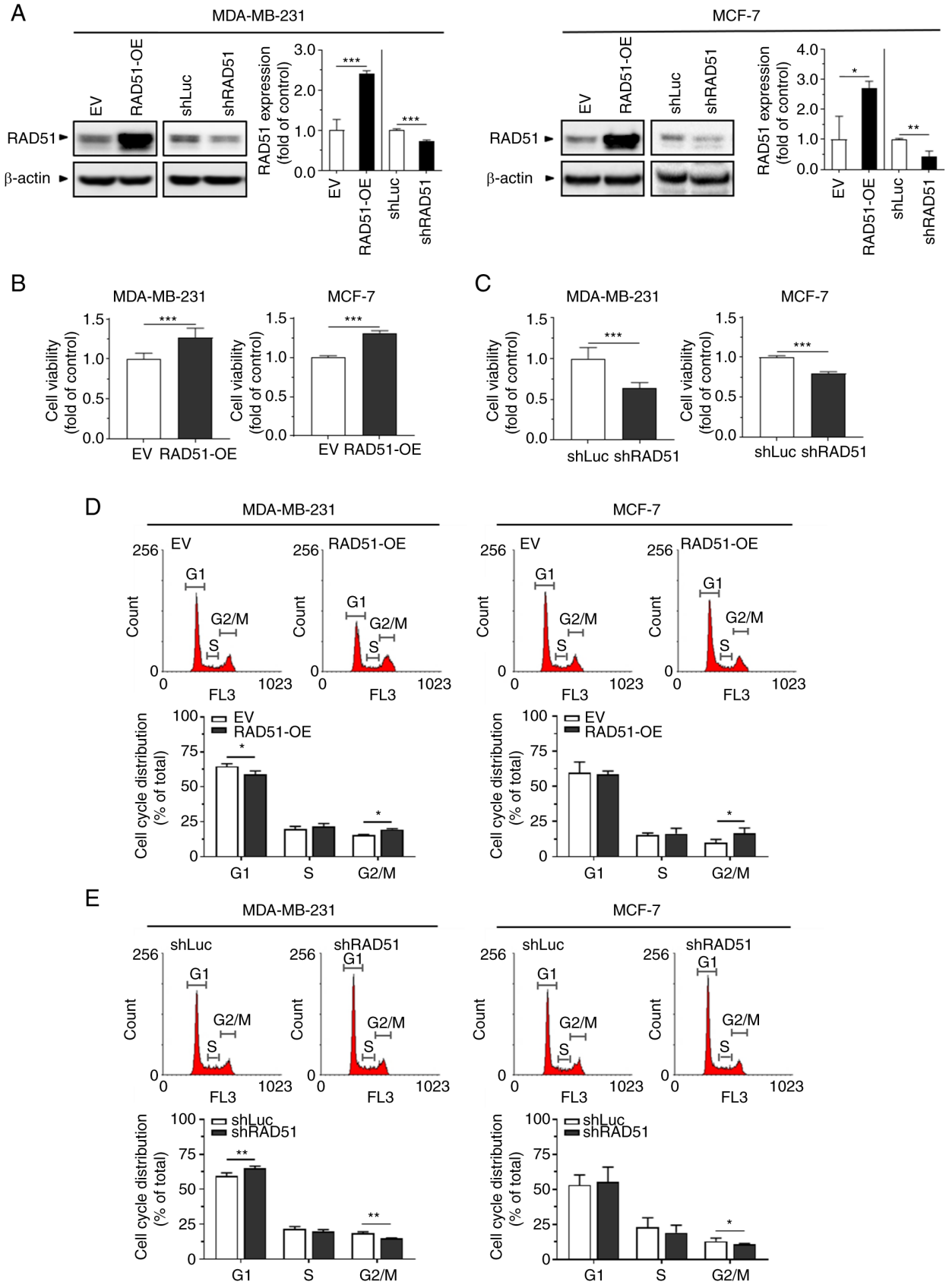

Figure 3. Effect of differential RAD51 expression on breast cancer cell growth and cell cycle distribution. (A) Protein expression in MDA-MB-231 and MCF-7 cells with overexpression of RAD51 or knockdown of RAD51 and their corresponding controls was analyzed by western blot. The blot images were created by Image Lab Software 6.1 (Bio-Rad Laboratories, Inc.). (B and C) MDA-MB-231 and MCF-7 cells with (B) overexpression of RAD51 or (C) knockdown of RAD51 and their corresponding controls were cultured for 72 h, followed by an XTT assay to examine cell viability. (D and E) MDA-MB-231 and MCF-7 cells with (D) overexpression of RAD51 or (E) knockdown of RAD51 and their corresponding controls were cultured until 80% confluence, followed by DNA staining with propidium iodide and flow cytometric analysis of the distribution of cell cycle phases. Values are presented as the mean ± standard deviation of three independent experiments. The P-values were determined by two-sided Student's t-test between the experimental and control groups. *P<0.05c; ***P<0.001. EV, empty vector; RAD51-OE, overexpression of RAD51; shLuc, knockdown of firefly luciferase; shRAD51, knockdown of RAD51.

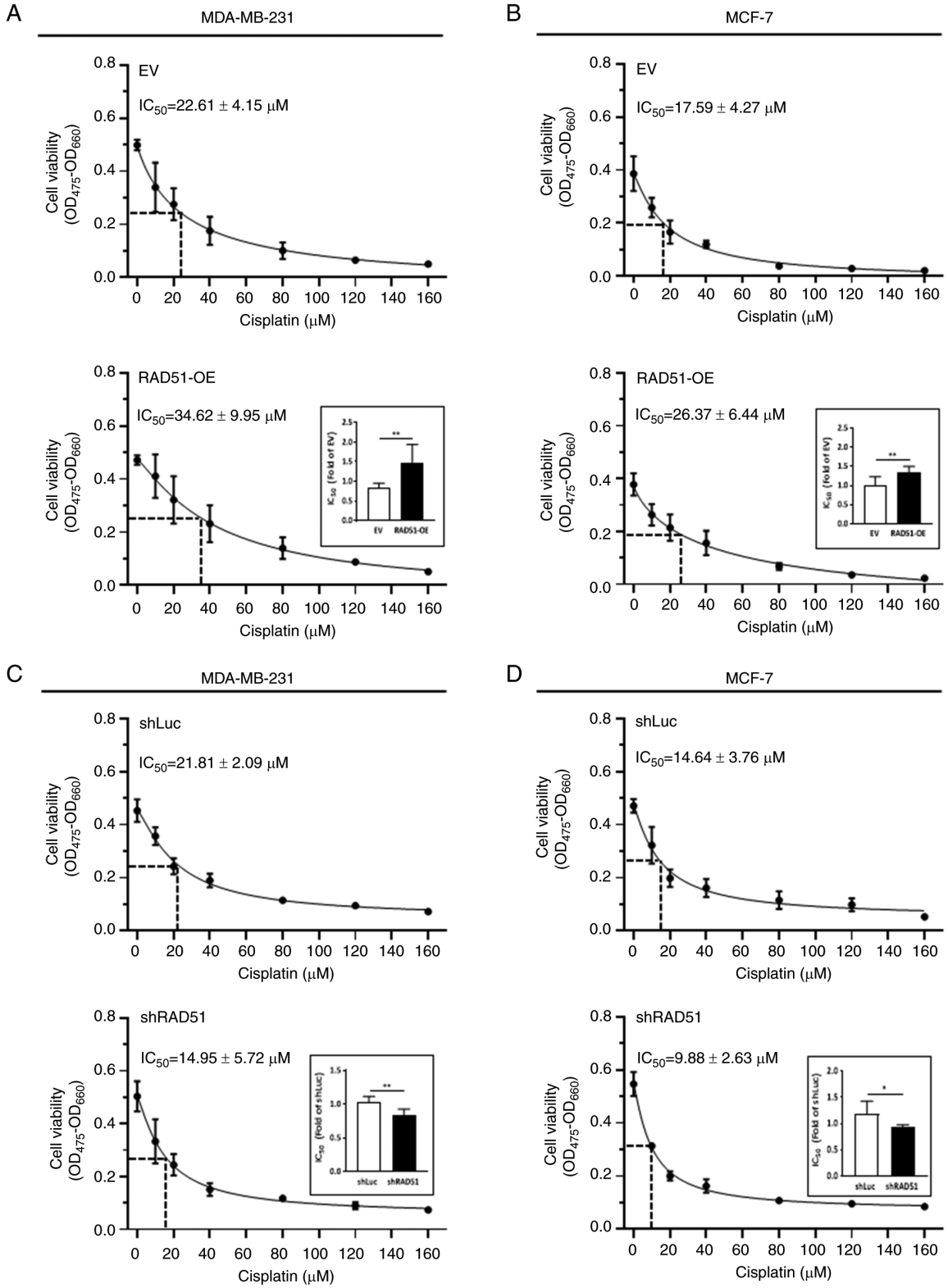

Figure 4. Effect of differential RAD51 expression on breast cancer cell growth with cisplatin treatment. (A) MDA-MB-231 and (B) MCF-7 cells with overexpression of RAD51 and (C) MDA-MB-231 and (D) MCF-7 cells with knockdown of RAD51 and their corresponding controls were treated with cisplatin (0-160 μM) for 72 h, followed by XTT assay for the measurement of the half-maximal inhibitory concentration indicated by dashed lines. Data are presented as the mean ± standard deviation from three triplicates for each condition, and similar results were obtained from two independent experiments. The P-values were determined by two-sided Student's t-test between experimental and control groups as shown in the insets. *P<0.05; **P<0.01. IC_{50}, half-maximal inhibitory concentration; EV, empty vector; RAD51-OE, overexpression of RAD51; shLuc, knockdown of firefly luciferase; shRAD51, knockdown of RAD51; OD, optical density.

a clearly stained band was shown above and near the molecular weight of 40 kDa in the cytoplasmic fraction of RAD51-overexpressing MDA-MB-231 cells, while there was no clear band in the nuclear fraction of RAD51-overexpressing MDA-MB-231 cells or control cells (Fig. S2B), suggesting the presence of a substantial protein interaction between

cytoplasmic RAD51 and the co-immunoprecipitated protein. Identification of the protein sequences for this particular band by LC-MS/MS revealed that it matched the sequences of β-actin (Fig. S2C), the major cytoplasmic isoform of the actin family expressed in non-muscle cells (30). As β-actin is the essential subunit of globular actin that forms F-actin in control of various types of cell growth and motility (30-32), the potential of the protein interaction between RAD51 and F-actin was further examined using breast cancer cell models in the present study. As indicated in Fig. 5D, overexpression of RAD51 in MDA-MB-231 cells did not affect the endogenous amount of F-actin expression. However, immunoprecipitation with anti-F-actin antibodies revealed that RAD51 was more abundantly co-immunoprecipitated in RAD51-overexpressing MDA-MB-231 cells compared to control cells (Fig. 5E). The increased protein interaction between RAD51 and F-actin was also evidenced by immunofluorescence, where RAD51-overexpressing MDA-MB-231 cells showed higher abundance of co-localization between RAD51 and F-actin compared to control cells (Fig. 5F). These results together suggest that alteration of RAD51 expression was associated with the migration and invasion ability of breast cancer cells, and the interaction between cytoplasmic RAD51 and actin filaments was potentially an association factor on these biological activities, which warrants further investigation.

Discussion

RAD51 represents one of the potential DNA damage repair-associated therapeutic candidates in breast cancer (8,33). However, the bilocation nature of RAD51 distributed in both the cytoplasm and the cell nucleus suggests that its role may extend further beyond DNA damage repair (13,15-17,34). In the present study, the differential expression of subcellular RAD51 in breast tumors revealed that elevated expression of cytoplasmic RAD51 was associated with adverse breast cancer progression and clinical outcomes, including increased cancer stage, grade, tumor size, LN metastasis, as well as poor disease-free and overall survival. In addition, elevated expression of cytoplasmic RAD51 in breast tumors was associated with poor disease-free and overall survival in the patients who received adjuvant chemotherapy, but this association was not significant in those without adjuvant chemotherapy. By contrast, elevated expression of nuclear RAD51 in breast tumors showed an opposite role for these clinical outcomes in comparison to cytoplasmic RAD51. The present clinical data support the notion of a distinct role between these two subcellular localizations of RAD51 in breast cancer progression and prognosis (16,17). Stratification of patient groups according to differential subcellular RAD51 location may therefore allow a more personalized approach to breast cancer evaluation.

Manipulation of the RAD51 expression level in human breast cancer cell lines has unveiled several roles of RAD51 in cancer cell growth and metastatic ability (35,36). For instance, knockdown of RAD51 in MDA-MB-231 cells was shown to reduce cell migration ability, whereas overexpression of RAD51 in BT549 and Hs578T cells promoted cell migration (14). In addition, increased chemoresistance to the poly(ADP-ribose) polymerase (PARP) inhibitor ABT-888 (Veliparib) (37) was observed in RAD51-overexpressing Hs578T cells (38). Another study using a brain metastasis-favored MDA-MB-231 subline, MDA-MB-231-BR (39), with RAD51 overexpression showed resistant phenotypes following chemotherapeutic treatment with doxorubicin (40). Furthermore, knockdown of RAD51 restored treatment sensitivity with HER2-targeted trastuzumab (Herceptin) (41) in SKBR3 and JIMT-1 cells (42). The current *in vitro* data using MDA-MB-231 and MCF-7 cells further unveiled that overexpression of RAD51 promoted malignant behaviors in these breast cancer cells, including enhanced cell growth with progressive G2/M cell cycle accumulation, enhanced metastatic ability in a Transwell migration assay and invadopodial invasion, and resistance to chemotherapeutic treatment with cisplatin. On the contrary, knockdown of RAD51 suppressed the malignant behaviors in MDA-MB-231 and MCF-7 cells. These results provide further evidence for the pro-oncogenic effect of RAD51 on breast cancer cells. Whether the differential RAD51 expression also affects treatment responses to first-line chemotherapeutic agents for breast cancer, such as anthracyclines and taxanes, warrants further investigation. In addition, caution should be taken regarding the potential off-target effects resulting from the application of shRNA, which may be further evaluated by additional experiments with the use of shRNA sequences against other coding regions of RAD51 for comparison. The complementation experiments by re-expressing RAD51 in breast cancer cells carrying knockdown of RAD51 may also be applied to demonstrate the specificity of shRNA. Furthermore, while the effect of differential RAD51 expression on breast cancer cell growth was examined by XTT assay in the current study, application of another approach to assess cell growth, such as measurement of the doubling time by direct counting of the cell number, may further confirm the results derived from this study.

Genomic instability is a hallmark of cancer, resulting from dysregulated DNA damage repair (43-45). The involvement of RAD51 in breast cancer progression may depend on its subcellular localization, with high cytoplasmic RAD51 or low nuclear RAD51 in breast tumors associated with poorer clinical outcomes, as shown in the present study and previous reports (16,17). An explanation for these clinical observations may relate to RAD51 translocation from the cell nucleus to the cytoplasm, hence the enhancement of genomic instability due to inappropriate DNA damage repair (Fig. 5G). For instance, the localization of RAD51 and BRCA1, a RAD51-interacting protein (46), was found to increase in the cytoplasm of breast cancer cells via activation of AKT signaling, leading to a phenotype of reduced nuclear localization of these two proteins and decreased DNA damage repair ability (47). The subcellular localization of RAD51 has been shown to be associated with multiple RAD51-interacting proteins, including BRCA1/2 (46,48,49) and RAD51 paralog RAD51C (50). Of note, RAD51 does not contain a nuclear localization signal (NLS) but a nuclear export signal (NES), and therefore, its nuclear translocation relies on the NLS-containing interaction proteins, such as BRCA1/2 and RAD51C (28,46,51). The presence of NES on RAD51 may partly explain the abundance of RAD51 in the cytoplasm of cancer cells expressing mutated BRCA, which commonly shows compromised nuclear localization of both BRCA and RAD51, leading to genomic instability (52). In addition, the NES of RAD51

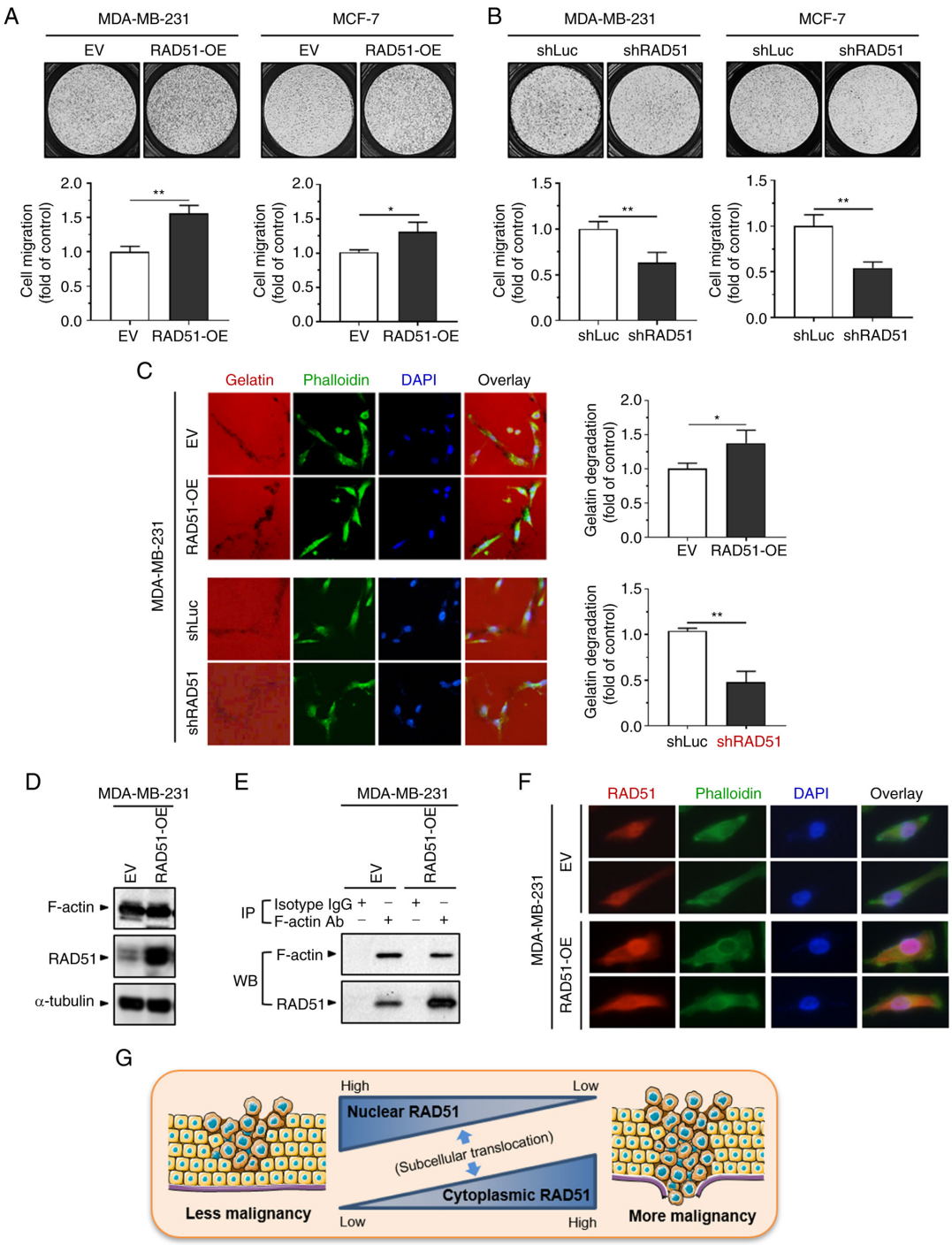

Figure 5. Effect of differential RAD51 expression on breast cancer cell migration and invasion, and the protein interaction with F-actin. MDA-MB-231 and MCF-7 cells with (A) overexpression of RAD51 or (B) knockdown of RAD51 and their corresponding controls were cultured for 24 h in Transwell inserts, followed by the procedures of the Transwell migration assay. The cell images were generated by NIS-Elements Imaging Software 5.0 (Nikon Corp.). (C) MDA-MB-231 cells with overexpression of RAD51 or knockdown of RAD51 and their corresponding controls were cultured for 24 h on glass chamber slides pre-coated with Cy3-conjugated gelatin (red), followed by the procedures of the invadopodial invasion assay. FITC-conjugated phalloidin (green) and DAPI (blue) were applied to detect F-actin and the cell nucleus, respectively (magnification, x200). Data were presented as the mean ± standard deviation from three independent experiments. P-values were determined by two-sided Student's t-test between experimental and control groups. *P<0.05; **P<0.01s. The cell images were created by AxioVision Software 4.8 (Carl Zeiss GmbH). (D) The protein expression in MDA-MB-231 cells with overexpression of RAD51 and their controls was analyzed by western blot. (E) Immunoprecipitation with anti-F-actin antibodies or isotype IgG was performed using the protein extracts of MDA-MB-231 cells with overexpression of RAD51 and their controls, followed by western blot analysis of the protein expression. The blot images were created by Image Lab Software 6.1 (Bio-Rad Laboratories, Inc.). (F) Immunofluorescence with anti-RAD51 antibodies was conducted on MDA-MB-231 cells with overexpression of RAD51 and their controls. Alexa Fluor 555-conjuagted donkey polyclonal antibodies against rabbit IgG was applied to detect RAD51 (red), and FITC-conjugated phalloidin (green) and DAPI (blue) were applied to detect F-actin and the cell nucleus, respectively. The cell images were created by AxioVision Software 4.8 (Carl Zeiss GmbH) (magnification, x400). (G) Schematic diagram of the impact of cytoplasmic vs. nuclear RAD51 on breast cancer malignancy. The current study suggests a pro-oncogenic role of cytoplasmic RAD51 in breast cancer progression. On the other hand, the canonical role of nuclear RAD51 in DNA damage repair may prevent breast tumors from further malignant transformation caused by genomic instability. The differential impact of subcellular RAD51 on breast malignancy may result from the translocation of RAD51 that occurs in a dynamic manner regulated by a network of RAD51 interaction proteins, such as BRCA1/2 and RAD51C. EV, empty vector; RAD51-OE, overexpression of RAD51; shLuc, knockdown of firefly luciferase; shRAD51, knockdown of RAD51; F-actin, filamentous actin; Ab, antibody; IP, immunoprecipitation; WB, western blot.

can be specifically masked when interacting with intact BRCA2 to retain itself in the cell nucleus, suggesting that the nuclear RAD51 concertedly participates in the BRCA tumor suppressor network via protein interactions (51,53).

In contrast to nuclear RAD51, the biological activity of cytoplasmic RAD51 has remained largely elusive. In the present study, β-actin was identified as a novel RAD51-interacting protein, and this protein interaction occurred in particular within the subcellular localization of cytoplasmic RAD51. Evidence was also provided to show that overexpression of RAD51 resulted in an increase of invadopodia, an F-actin-based cytoskeletal remodeling for cancer invasion (54), and that overexpression of RAD51 co-localized with F-actin in the cytoplasm of breast cancer cells. β-Actin has been shown to be the monomeric component for F-actin formation and the process is intricately regulated by a number of actin interaction proteins, as alteration of F-actin formation may have a critical influence on cancer progression and metastasis (32,55,56). The current findings not only add cytoplasmic RAD51 and β-actin to the growing pool of protein-protein interaction, but also raise the possibility for a potential role of the protein interaction between cytoplasmic RAD51 and actin filaments in breast cancer. Future studies are required to elucidate whether alteration of this protein interaction impinges on breast cancer cell malignancy.

In the current study, one limitation is that the role of overall RAD51 expression but not changes in the subcellular location of RAD51 was examined in the *in vitro* experiments. RAD51 itself has no NLS and its subcellular localization is influenced by its interaction with other proteins, including BRCA1/2 (46,48,49) and RAD51 paralog RAD51C (50). To avoid the inconclusive result from manipulation of subcellular localization of RAD51 by overexpression or downregulation of BRCA1/2 or RAD51C, adding NLS to the RAD51 gene to manipulate its subcellular localization may be an alternative approach. Another limitation is that the majority of patients recruited in the present study received adjuvant chemotherapy, leading to a significantly reduced observation number for those without adjuvant chemotherapy. Therefore, further increments of the observation number for patients without adjuvant chemotherapy are required to confirm the prognostic role of subcellular RAD51 in this population of patients with breast cancer. Furthermore, simultaneous evaluation of RAD51 expression in the cytoplasmic and nuclear localization may provide additional information for the prognostic role of subcellular RAD51. For instance, future studies may consider analyzing treatment outcomes according to both subcellular RAD51 expression levels, such as $cyto^{high}/nu^{low}$ vs. $cyto^{low}/nu^{high}$ of RAD51 expression in patients with breast cancer. The third limitation of the present study is that the effect of cisplatin treatment on the subcellular location of RAD51 and the interaction between cytoplasmic RAD51 and F-actin in transfected cells was not investigated and is worthy of further investigation in a future study.

For future recommendations, with the increasing use of PARP inhibitors in cancer treatment, there is an unmet clinical need to implement homologous recombination deficiency (HRD) testing in clinical practice. In the coming years, RAD51 recombinase protein may offer additional dimensions by functioning as a biomarker for HRD tests (57).

In conclusion, in the present study, the role of subcellular RAD51 in breast cancer was evaluated by clinical measurements, unveiling that elevated cytoplasmic RAD51 expression was associated with adverse clinicopathologic features and outcomes for the patients, whereas elevated nuclear RAD51 expression had the inverse effect on these clinical parameters. The results of the *in vitro* investigation were in accordance with the cancer-promoting effect of RAD51, where the malignant behaviors of breast cancer cells were enhanced by overexpression of RAD51 but repressed by knockdown of RAD51. These findings together suggest a pro-oncogenic role of cytoplasmic RAD51 in contrast to nuclear RAD51, which may provide insight for the further development of therapeutic strategies for breast cancer. For instance, stratification of patients with breast cancer by differential subcellular RAD51 expression may benefit them in terms of chemotherapeutic selection and improvement of personalized prognosis.

Acknowledgements

The analysis of clinical data was performed with the assistance of Dr Yi-Chen Lee (Department of Anatomy, School of Medicine, Kaohsiung Medical University, Kaohsiung, Taiwan). Dr Shyh-Horng Chiou (Quantitative Proteomics Center, Center for Research Resources and Development, Kaohsiung Medical University, Kaohsiung, Taiwan) performed the LC-MS/MS analysis. The schematic presented in Fig. 5G was generated using the illustration elements from Servier Medical Art (https://smart.servier.com), which is in compliance with the terms of the Creative Commons Attribution 3.0 Unported License (https://creativecommons.org/licenses/by/3.0/).

Funding

This work was supported by grants from the National Science and Technology Council (grant nos. NSTC 112-2314-B-037-120 and NSTC 112-2314-B-037-112-MY3) and Center for Intelligent Drug Systems and Smart Bio-devices (IDS^2B) from the Featured Areas Research Center Program within the framework of the Higher Education Sprout Project by the Ministry of Education in Taiwan. This work was also supported by grants from Kaohsiung Medical University Hospital [grant nos. KMUH110-0R43, KMUH111-1R37, KMUH-DK(A)110001 and KMUH-DK(A)112001] and Kaohsiung Medical University [grant nos. KMU-DK(A)111005, KMU-DK(A)112006, NYCU-KMU-111-I002, NYCU-KMU-112-I005, NSYSU-KMU-112-P04, KMU-TC112A03-5], Taiwan.

Availability of data and materials

The datasets used and/or analyzed during the current study are available from the corresponding author on reasonable request.

Authors' contributions

YYW, KHC, ACH, SL, PYC, YCW, MFH and SSFY conceived and designed the study. YYW, KHC, ACH, PYC and SSFY performed the experiments. YYW, ACH, SL, YCW, MFH, and SSFY analyzed and interpreted the data. YYW, KHC and

ACH wrote the manuscript. SL, PYC, YCW, MFH and SSFY critically revised the manuscript. YYW and SSFY confirm the authenticity of all the raw data. All authors have reviewed and approved the final manuscript.

Ethics approval and consent to participate

The study was approved by the Institutional Review Board of Kaohsiung Medical University Hospital [Kaohsiung, Taiwan; approval no. KMUH-IRB-20130031 and KMUHIRB-E(I)-20180136] and conducted in accordance with the Declaration of Helsinki. All of the samples used in the present study were de-identified samples from the hospital's biobank added with the informed consent of the patients, but the requirement of informed consent to include them in the present study was waived by the ethics committee.

Patient consent for publication

Not applicable.

Competing interests

The authors declare that they have no competing interests.

References

1. Sung H, Ferlay J, Siegel RL, Laversanne M, Soerjomataram I, Jemal A and Bray F: Global cancer statistics 2020: GLOBOCAN estimates of incidence and mortality worldwide for 36 cancers in 185 countries. CA Cancer J Clin 71: 209-249, 2021.
2. Moo TA, Sanford R, Dang C and Morrow M: Overview of breast cancer therapy. PET Clin 13: 339-354, 2018.
3. Trayes KP and Cokenakes SEH: Breast cancer treatment. Am Fam Physician 104: 171-178, 2021.
4. Martinez-Perez C, Turnbull AK, Ekatah GE, Arthur LM, Sims AH, Thomas JS and Dixon JM: Current treatment trends and the need for better predictive tools in the management of ductal carcinoma in situ of the breast. Cancer Treat Rev 55: 163-172, 2017.
5. Fahad Ullah M: Breast cancer: Current perspectives on the disease status. Adv Exp Med Biol 1152: 51-64, 2019.
6. Giridhar KV and Liu MC: Available and emerging molecular markers in the clinical management of breast cancer. Expert Rev Mol Diagn 19: 919-928, 2019.
7. Nickoloff JA: Targeting replication stress response pathways to enhance genotoxic chemo- and radiotherapy. Molecules 27: 4736, 2022.
8. Wang Z, Jia R, Wang L, Yang Q, Hu X, Fu Q, Zhang X, Li W and Ren Y: The emerging roles of Rad51 in cancer and its potential as a therapeutic target. Front Oncol 12: 935593, 2022.
9. Lee MG, Lee KS and Nam KS: The association of changes in RAD51 and survivin expression levels with the proton beam sensitivity of Capan-1 and Panc-1 human pancreatic cancer cells. Int J Oncol 54: 744-752, 2019.
10. Connell PP, Jayathilaka K, Haraf DJ, Weichselbaum RR, Vokes EE and Lingen MW: Pilot study examining tumor expression of RAD51 and clinical outcomes in human head cancers. Int J Oncol 28: 1113-1119, 2006.
11. Luzhna L, Golubov A, Ilnytskyy S, Chekhun VF and Kovalchuk O: Molecular mechanisms of radiation resistance in doxorubicin-resistant breast adenocarcinoma cells. Int J Oncol 42: 1692-1708, 2013.
12. Maacke H, Opitz S, Jost K, Hamdorf W, Henning W, Krüger S, Feller AC, Lopens A, Diedrich K, Schwinger E and Stürzbecher HW: Over-expression of wild-type Rad51 correlates with histological grading of invasive ductal breast cancer. Int J Cancer 88: 907-913, 2000.
13. Hu J, Wang N and Wang YJ: XRCC3 and RAD51 expression are associated with clinical factors in breast cancer. PLoS One 8: e72104, 2013.
14. Wiegmans AP, Al-Ejeh F, Chee N, Yap PY, Gorski JJ, Da Silva L, Bolderson E, Chenevix-Trench G, Anderson R, Simpson PT, *et al*: Rad51 supports triple negative breast cancer metastasis. Oncotarget 5: 3261-3272, 2014.
15. Soderlund K, Skoog L, Fornander T and Askmalm MS: The BRCA1/BRCA2/Rad51 complex is a prognostic and predictive factor in early breast cancer. Radiother Oncol 84: 242-251, 2007.
16. Sosinska-Mielcarek K, Duchnowska R, Winczura P, Badzio A, Majewska H, Lakomy J, Pęksa R, Pieczyńska B, Radecka B, Dębska S, *et al*: Immunohistochemical prediction of brain metastases in patients with advanced breast cancer: The role of Rad51. Breast 22: 1178-1183, 2013.
17. Alshareeda AT, Negm OH, Aleskandarany MA, Green AR, Nolan C, TigHhe PJ, Madhusudan S, Ellis IO and Rakha EA: Clinical and biological significance of RAD51 expression in breast cancer: A key DNA damage response protein. Breast Cancer Res Treat 159: 41-53, 2016.
18. Chiu WC, Fang PT, Lee YC, Wang YY, Su YH, Hu SC, Chen YK, Tsui YT, Kao YH, Huang MY and Yuan SF: DNA Repair Protein Rad51 induces tumor growth and metastasis in esophageal squamous cell carcinoma via a p38/Akt-Dependent pathway. Ann Surg Oncol 27: 2090-2101, 2020.
19. Yuan SS, Hou MF, Hsieh YC, Huang CY, Lee YC, Chen YJ and Lo S: Role of MRE11 in cell proliferation, tumor invasion, and DNA repair in breast cancer. J Natl Cancer Inst 104: 1485-1502, 2012.
20. Liu Y, Lu LL, Wen D, Liu DL, Dong LL, Gao DM, Bian XY, Zhou J, Fan J and Wu WZ: MiR-612 regulates invadopodia of hepatocellular carcinoma by HADHA-mediated lipid reprogramming. J Hematol Oncol 13: 12, 2020.
21. Lee MY, Huang CH, Kuo CJ, Lin CL, Lai WT and Chiou SH: Clinical proteomics identifies urinary CD14 as a potential biomarker for diagnosis of stable coronary artery disease. PLoS One 10: e0117169, 2015.
22. Cottrell JS: Protein identification using MS/MS data. J Proteomics 74: 1842-1851, 2011.
23. Nedeljkovic M and Damjanovic A: Mechanisms of chemotherapy resistance in triple-negative breast cancer-how we can rise to the challenge. Cells 8: 957, 2019.
24. Prihantono and Faruk M: Breast cancer resistance to chemotherapy: When should we suspect it and how can we prevent it? Ann Med Surg 70: 102793, 2021.
25. Holliday DL and Speirs V: Choosing the right cell line for breast cancer research. Breast Cancer Res 13: 215, 2011.
26. Dasari S and Tchounwou PB: Cisplatin in cancer therapy: Molecular mechanisms of action. Eur J Pharmacol 740: 364-378, 2014.
27. Guney Eskiler G, Sahin E, Deveci Ozkan A, Cilingir Kaya OT and Kaleli S: Curcumin induces DNA damage by mediating homologous recombination mechanism in triple negative breast cancer. Nutr Cancer 72: 1057-1066, 2020.
28. Gildemeister OS, Sage JM and Knight KL: Cellular redistribution of Rad51 in response to DNA damage: Novel role for Rad51C. J Biol Chem 284: 31945-31952, 2009.
29. Mladenov E, Anachkova B and Tsaneva I: Sub-nuclear localization of Rad51 in response to DNA damage. Genes Cells 11: 513-524, 2006.
30. Dugina VB, Shagieva GS and Kopnin PB: Biological role of actin isoforms in mammalian cells. Biochemistry 84: 583-592, 2019.
31. Bunnell TM, Burbach BJ, Shimizu Y and Ervasti JM: β-Actin specifically controls cell growth, migration, and the G-actin pool. Mol Biol Cell 22: 4047-4058, 2011.
32. Suresh R and Diaz RJ: The remodelling of actin composition as a hallmark of cancer. Transl Oncol 14: 101051, 2021.
33. Gourley C, Balmana J, Ledermann JA, Serra V, Dent R, Loibl S, Pujade-Lauraine E and Boulton SJ: Moving from poly (ADP-ribose) polymerase inhibition to targeting DNA repair and DNA damage response in cancer therapy. J Clin Oncol 37: 2257-2269, 2019.
34. Honrado E, Osorio A, Palacios J, Milne RL, Sánchez L, Díez O, Cazorla A, Syrjakoski K, Huntsman D, Heikkilä P, *et al*: Immunohistochemical expression of DNA repair proteins in familial breast cancer differentiate BRCA2-associated tumors. J Clin Oncol 23: 7503-7511, 2005.
35. Klein HL: The consequences of Rad51 overexpression for normal and tumor cells. DNA Repair 7: 686-693, 2008.
36. Gachechiladze M, Skarda J, Soltermann A and Joerger M: RAD51 as a potential surrogate marker for DNA repair capacity in solid malignancies. Int J Cancer 141: 1286-1294, 2017.

37. Stodtmann S, Nuthalapati S, Eckert D, Kasichayanula S, Joshi R, Bach BA, Mensing S, Menon R and Xiong H: A population pharmacokinetic meta-analysis of veliparib, a PARP inhibitor, across phase 1/2/3 trials in cancer patients. J Clin Pharmacol 61: 1195-1205, 2021.
38. Wiegmans AP, Yap PY, Ward A, Lim YC and Khanna KK: Differences in expression of key DNA damage repair genes after epigenetic-Induced BRCAness dictate synthetic lethality with PARP1 inhibition. Mol Cancer Ther 14: 2321-2331, 2015.
39. Yoneda T, Williams PJ, Hiraga T, Niewolna M and Nishimura R: A bone-seeking clone exhibits different biological properties from the MDA-MB-231 parental human breast cancer cells and a brain-seeking clone in vivo and in vitro. J Bone Miner Res 16: 1486-1495, 2001.
40. Woditschka S, Evans L, Duchnowska R, Reed LT, Palmieri D, Qian Y, Badve S, Sledge G Jr, Gril B, Aladjem MI, *et al*: DNA double-strand break repair genes and oxidative damage in brain metastasis of breast cancer. J Natl Cancer Inst 106: dju145, 2014.
41. Wang J and Xu B: Targeted therapeutic options and future perspectives for HER2-positive breast cancer. Signal Transduct Target Ther 4: 34, 2019.
42. Nam S, Chang HR, Jung HR, Gim Y, Kim NY, Grailhe R, Seo HR, Park HS, Balch C, Lee J, *et al*: A pathway-based approach for identifying biomarkers of tumor progression to trastuzumab-resistant breast cancer. Cancer Lett 356: 880-890, 2015.
43. Negrini S, Gorgoulis VG and Halazonetis TD: Genomic instability-an evolving hallmark of cancer. Nat Rev Mol Cell Biol 11: 220-228, 2010.
44. Schild D and Wiese C: Overexpression of RAD51 suppresses recombination defects: A possible mechanism to reverse genomic instability. Nucleic Acids Res 38: 1061-1070, 2010.
45. Chen CC, Feng W, Lim PX, Kass EM and Jasin M: Homology-directed repair and the role of BRCA1, BRCA2, and related proteins in genome integrity and cancer. Annu Rev Cancer Biol 2: 313-336, 2018.
46. Scully R, Xie A and Nagaraju G: Molecular functions of BRCA1 in the DNA damage response. Cancer Biol Ther 3: 521-527, 2004.
47. Plo I, Laulier C, Gauthier L, Lebrun F, Calvo F and Lopez BS: AKT1 inhibits homologous recombination by inducing cytoplasmic retention of BRCA1 and RAD51. Cancer Res 68: 9404-9412, 2008.
48. Yuan SS, Lee SY, Chen G, Song M, Tomlinson GE and Lee EY: BRCA2 is required for ionizing radiation-induced assembly of Rad51 complex in vivo. Cancer Res 59: 3547-3551, 1999.
49. Davies AA, Masson JY, McIlwraith MJ, Stasiak AZ, Stasiak A, Venkitaraman AR and West SC: Role of BRCA2 in control of the RAD51 recombination and DNA repair protein. Mol Cell 7: 273-282, 2001.
50. Suwaki N, Klare K and Tarsounas M: RAD51 paralogs: Roles in DNA damage signalling, recombinational repair and tumorigenesis. Semin Cell Dev Biol 22: 898-905, 2011.
51. Jeyasekharan AD, Liu Y, Hattori H, Pisupati V, Jonsdottir AB, Rajendra E, Lee M, Sundaramoorthy E, Schlachter S, Kaminski CF, *et al*: A cancer-associated BRCA2 mutation reveals masked nuclear export signals controlling localization. Nat Struct Mol Biol 20: 1191-1198, 2013.
52. Paul A and Paul S: The breast cancer susceptibility genes (BRCA) in breast and ovarian cancers. Front Biosci 19: 605-618, 2014.
53. Zhao W, Wiese C, Kwon Y, Hromas R and Sung P: The BRCA tumor suppressor network in chromosome damage repair by homologous recombination. Annu Rev Biochem 88: 221-245, 2019.
54. Paterson EK and Courtneidge SA: Invadosomes are coming: New insights into function and disease relevance. FEBS J 285: 8-27, 2018.
55. Izdebska M, Zielinska W, Grzanka D and Gagat M: The role of actin dynamics and actin-binding proteins expression in epithelial-to-mesenchymal transition and its association with cancer progression and evaluation of possible therapeutic targets. Biomed Res Int 2018: 4578373, 2018.
56. Nersesian S, Williams R, Newsted D, Shah K, Young S, Evans PA, Allingham JS and Craig AW: Effects of modulating actin dynamics on HER2 cancer cell motility and metastasis. Sci Rep 8: 17243, 2018.
57. van Wijk LM, Nilas AB, Vrieling H and Vreeswijk MPG: RAD51 as a functional biomarker for homologous recombination deficiency in cancer: A promising addition to the HRD toolbox? Expert Rev Mol Diagn 22: 185-199, 2022.